

# Formation of a Stacked Dimeric G-Quadruplex Containing Bulges by the 5'-Terminal Region of Human Telomerase RNA (hTERC)

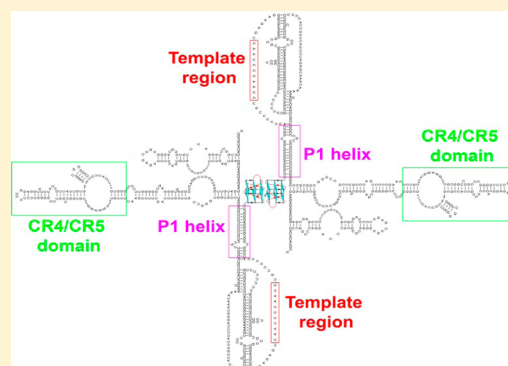
Herry Martadinata<sup>†,‡</sup> and Anh Tuân Phan<sup>\*,†</sup>

<sup>†</sup>School of Physical and Mathematical Sciences, Nanyang Technological University, Singapore 637371

<sup>‡</sup>School of Biological Sciences, Nanyang Technological University, Singapore 637551

## S Supporting Information

**ABSTRACT:** We investigate the structure formed by the first 18-nt of the 5'-terminal region of the human telomerase RNA (hTERC or hTR) using gel electrophoresis and UV, CD, and NMR spectroscopy. Our data suggest that this 18-nt sequence, r(GGGUUGCGGAGGGUGGGC), can form a stacked dimeric G-quadruplex in potassium solution. The two subunits, each being a three-layer parallel-stranded G-quadruplex with a cytosine bulge, are stacked at their 5'-end. The formation of this stacked dimeric G-quadruplex containing bulges could be biologically relevant for the dimerization and other interactions of the active human telomerase.



Nucleic acid G-quadruplexes are four-stranded structures formed by sequences containing stretches of guanines through the stacking of G·G·G·G tetrads and are stabilized by cations such as K<sup>+</sup> or Na<sup>+</sup>.<sup>1–3</sup> For example, a DNA or RNA fragment containing four G-tracts separated by short linkers could fold into an intramolecular G-quadruplex in physiological ionic conditions. G-quadruplexes are polymorphic with regard to strand orientations, loops, and glycosidic conformations of guanine bases.<sup>1–4</sup> The formation of bulges,<sup>5,6</sup> snapback motifs,<sup>7–9</sup> and other additional structural elements<sup>10–18</sup> increases the complexity of possible G-quadruplex structures. G-Quadruplexes can also form higher-order structures through stacking<sup>19–23</sup> or interlocking<sup>24–29</sup> of multiple G-quadruplex units. In contrast to the DNA counterparts, which were shown to adopt various G-quadruplex topologies with different loop types and strand orientations as well as mixtures of *syn* and *anti* guanines,<sup>1–4</sup> only a few RNA G-quadruplex structures were reported, and they were observed only in the parallel conformation with *anti* guanines.<sup>21,29–35</sup> However, high structural complexity was still observed in a recent example of an RNA aptamer bound to a FMRP peptide.<sup>35</sup> Increasing evidence has recently been reported for the formation and biological relevance of DNA and RNA G-quadruplexes in the cells.<sup>36–40</sup>

In most (80–85%) cancer cells, the enzyme telomerase<sup>41</sup> is up-regulated for telomere maintenance.<sup>42</sup> Telomerase, consisting of a catalytic protein subunit TERT and an RNA template subunit TERC (or TR), acts as a reverse transcriptase to add telomeric repeats to the 3'-end telomere overhang.<sup>43,44</sup> The recently reported structure of the *Tetrahymena* telomerase<sup>45</sup> and that of the human telomerase<sup>46</sup> revealed the organization of different components within this holoenzyme. The active *in*

*vivo*-assembled human telomerase was recently observed as a dimer,<sup>46,47</sup> although some reports showed that human telomerase could also function as a monomer.<sup>48</sup> The secondary structure of TERC is conserved across many different species,<sup>49</sup> and the high-resolution structure of several domains of human telomerase RNA (hTERC) has been reported.<sup>50</sup> The 5'-terminal region (first 37 nucleotides) of hTERC contains several G-tracts with a total of 22 guanines (Figure S1, Supporting Information). In an earlier report on the secondary structure of hTERC, the 3' portion of this region (residues 18–37) containing 10 guanines was shown to participate in the formation of a P1 helix that defined the boundary for the reverse transcription template, while the structure of the extreme 5' portion (residues 1–17) containing 12 guanines was not proposed.<sup>49</sup> More recent reports showed that G-quadruplexes can be formed in the 5'-terminal region of hTERC, involving either only the extreme 5' portion<sup>51</sup> or also a part of the P1 helix.<sup>52</sup> G-Quadruplex formation at the extreme 5' portion can protect hTERC from degradation during telomerase biogenesis and maturation<sup>53</sup> or affect its interaction with another domain of hTERC called CR4/CR5,<sup>51</sup> while internal G-quadruplex formation involving a part of the P1 helix can interfere with this helix formation and affect correct template definition.<sup>52,54,55</sup> High-affinity interaction between potential G-quadruplexes formed in the 5'-terminal region of hTERC with the RHAU helicase has also been reported.<sup>53–55</sup>

Here, we study the structure formed by the first 18-nt of the 5'-terminal region of hTERC using gel electrophoresis and UV,

**Received:** November 25, 2013

**Revised:** February 16, 2014

**Published:** March 6, 2014

CD, and NMR spectroscopy. Our data suggest that this sequence can form a stacked dimeric G-quadruplex with bulges. This finding could have implications in the structure and function of the human telomerase.

## MATERIALS AND METHODS

**Sample Preparation.** RNA oligonucleotides used in this study were purchased from Research Instrument Pte Ltd. (Singapore) with PAGE purification. The samples were dissolved in solution containing (i) 70 mM KCl and 20 mM potassium phosphate at pH 7; or (ii) 5 mM potassium phosphate at pH 7; or (iii) 0.5 mM KCl and 0.5 mM potassium phosphate at pH 7. The samples were heated to 98 °C and left to cool down to room temperature overnight.

**Circular Dichroism.** CD spectra at 25 °C were recorded on a JASCO J-815 spectropolarimeter using a 1-mm path-length quartz cuvette in a reaction volume of 250  $\mu$ L. RNA concentration was 50  $\mu$ M. Scans from 220 to 320 nm were performed with 200-nm/min scanning speed. For each spectrum, an average of 5 scans was taken, and the spectral contribution from the buffer was subtracted. Thermal stability of the TER18-2A sequence r(AAGGGUUGCGGAGGGUUGGGC) was characterized in a CD melting experiment measured at 260 nm. RNA concentration was 50  $\mu$ M. The temperature ranged from 20 to 95 °C; cooling and heating experiments were performed with a ramping rate of 0.2 °C per min. Zero was taken as the baseline for the unfolded species.

**UV Melting.** Thermal stability of the hTERC sequence r(GGGUUGCGGAGGGUUGGGC) termed TER18 and human telomeric RNA (TERRA) sequence r(UAGGGUUAGGGUAGGGUUAGGGUUAGGGUU) in K<sup>+</sup> solution, containing various amounts of KCl, was characterized by UV melting experiments. The absorbance at 295 nm was measured as a function of temperature on a Jasco V-650 UV-vis spectrophotometer using quartz cuvettes with 1-mm or 1-cm path length. The data were zero-corrected using the baseline absorption measurement at 320 nm. RNA concentration was 5  $\mu$ M. The temperature ranged from 15 to 98 °C; cooling and heating experiments were performed with a ramping rate of 0.2 °C per min. The melting point ( $T_m$ ) was defined as the temperature where 50% of the sample was unfolded.

**Gel Electrophoresis.** Gel electrophoresis experiments were performed on native gel containing 20% polyacrylamide (acrylamide/bis-acrylamide = 37.5:1) in TBE buffer (pH 8.3). 40 mM KCl was added into the buffer and the gel to maintain the G-quadruplex structure formation. The gel was viewed by the UV-shadowing method.

**NMR Spectroscopy.** NMR experiments were performed on 600 and 700 MHz Bruker spectrometers, both equipped with a CryoProbe. Spectra were recorded at 25 °C, unless otherwise specified. The strand concentration of NMR samples was typically 50–400  $\mu$ M. For NMR experiments in H<sub>2</sub>O, JR-type pulse sequences were used for water signal suppression.<sup>56,57</sup> Samples for NMR experiments contained 90% H<sub>2</sub>O and 10% D<sub>2</sub>O.

## RESULTS AND DISCUSSION

**The First 18-nt Sequence at the 5'-Terminal Region of hTERC Forms a Stable Parallel-Stranded G-Quadruplex in Potassium Solution.** In this work, we examined the 18-nt sequence r(GGGUUGCGGAGGGUUGGGC) located at the 5'-end of human telomerase RNA, denoted as TER18. The CD

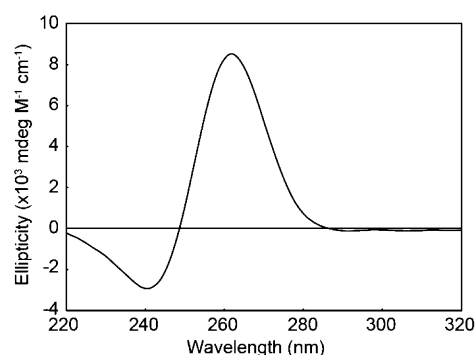


**Figure 1.** CD spectrum of the TER18 sequence r(GGGUUGCGG-AGGGUUGGGC) in solution containing 70 mM KCl and 20 mM potassium phosphate (pH 7) showing the formation of a parallel-stranded G-quadruplex. Experimental conditions: temperature, 25 °C; RNA strand concentration, 50  $\mu$ M.

**Table 1. Melting Temperature ( $T_m$ ) of G-Quadruplexes Formed by the TER18 and TERRA Sequences at Two Different Salt Concentrations<sup>a</sup>**

sequence	$T_m$ <sup>b</sup> (°C) at high salt conditions <sup>c</sup>	$T_m$ <sup>b</sup> (°C) at low salt conditions <sup>d</sup>
TER18	83.5 $\pm$ 0.5	68.0 $\pm$ 0.0
TERRA	80.0 $\pm$ 1.0	53.5 $\pm$ 0.0

<sup>a</sup>RNA concentration was 5  $\mu$ M. <sup>b</sup>The uncertainties ( $\pm$  values) indicate the hysteresis between heating and cooling curves. <sup>c</sup>The solution contained 70 mM KCl and 20 mM potassium phosphate (pH 7). <sup>d</sup>The solution contained 0.5 mM KCl and 0.5 mM potassium phosphate (pH 7).

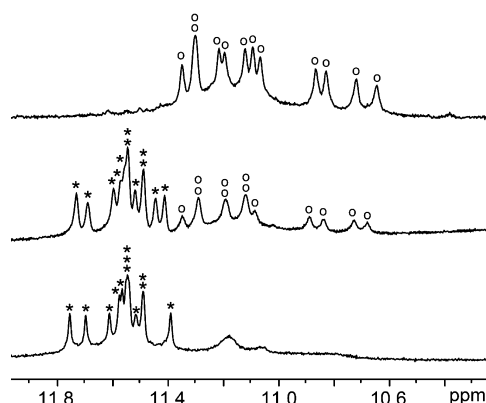


**Figure 2.** Imino proton spectra of TER18 in different salt conditions: 70 mM KCl and 20 mM potassium phosphate at pH 7 (top spectrum); 5 mM potassium phosphate at pH 7 (middle spectrum); 0.5 mM KCl and 0.5 mM potassium phosphate at pH 7 (bottom spectrum). Peaks of the two G-quadruplex conformations are marked by asterisks and circles, respectively. Experimental conditions: temperature, 25 °C; RNA concentration, 100  $\mu$ M.

spectrum of this sequence in K<sup>+</sup> solution shows a positive peak at 260 nm and a negative trough at 240 nm (Figure 1), which are the characteristics of the formation of a parallel-stranded G-quadruplex. Melting experiments (Figure S2, Supporting Information) indicate a higher thermal stability for the G-quadruplex formed by this sequence as compared to that formed by a four-repeat human TERRA sequence r-[(UAGGGU)<sub>4</sub>U] (Table 1). This behavior was observed at both high salt (70 mM KCl and 20 mM potassium phosphate at

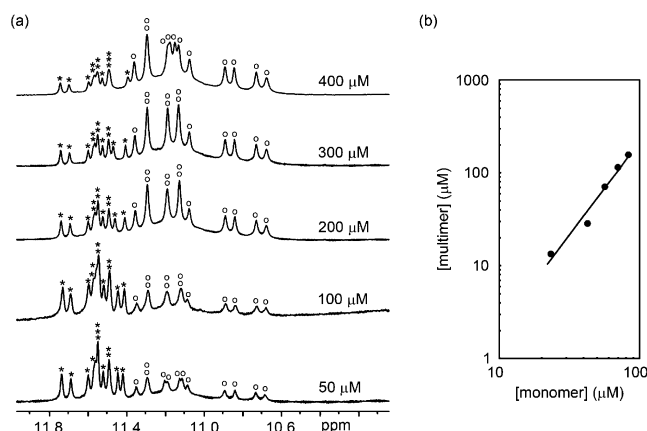


**Figure 3.** Effect of RNA concentration on the monomer–dimer equilibrium of TER18 G-quadruplexes at 25 °C in solution containing 5 mM potassium phosphate at pH 7. (a) Imino proton spectra of TER18 at RNA concentrations ranging from 50 to 400  $\mu\text{M}$ . The peaks marked by asterisks indicate the monomer population, while the peaks marked by circles indicate the dimer population. (b) Plot of the concentration of the dimer against that of the monomer as measured by NMR spectroscopy. Both axes are in logarithmic scale. A straight line of slope 2 is drawn across the data points.

pH 7) and low salt (0.5 mM KCl and 0.5 mM potassium phosphate at pH 7) conditions. The higher thermal stability of TER18 as compared with TERRA might be related to the shorter loop lengths in the former structure.

**Monomer–Dimer Equilibrium of TER18 G-Quadruplexes.** The imino proton NMR spectrum of the TER18 sequence (RNA concentration, 100  $\mu\text{M}$ ) in solution containing  $\sim 100$  mM  $\text{K}^+$  (70 mM KCl and 20 mM potassium phosphate at pH 7) shows 12 peaks at 10–12 ppm (marked with circles; top spectrum, Figure 2) indicating the formation of a well-defined G-quadruplex. The detection of 12 sharp imino protons suggests that all 12 guanines of the TER18 sequence participate in the G-tetrad core formation of this structure. At a lower  $\text{K}^+$  concentration (5 mM potassium phosphate at pH 7), a second set of 12 imino protons emerged along with the first set observed at the high-salt condition (labeled with asterisks and circles, respectively; middle spectrum, Figure 2), indicating the equilibrium between two G-quadruplex conformations. Formation of only the second G-quadruplex form was observed at a very low salt condition (0.5 mM KCl and 0.5 mM potassium phosphate at pH 7).

We examined the effect of RNA concentration (ranging from 50 to 400  $\mu\text{M}$ ) on the equilibrium between the two G-quadruplex forms of TER18 at 25 °C and 5 mM potassium phosphate solution at pH 7. Peaks from the two conformations

were observable across the RNA concentration range (Figure 3a). Increasing the RNA concentration shifted the equilibrium toward the conformation observed at high salt conditions, presumably a multimer. The plot of the equilibrium concentrations between the two forms in logarithmic scale shows a slope of  $\sim 2$  (Figure 3b), consistent with an equilibrium between monomer and dimer G-quadruplexes.<sup>56,57</sup>

**TER18 Forms a Stacked Dimeric G-Quadruplex Containing Bulges.** On the basis of the data described above as well as previous reports on bulge formation<sup>6</sup> and stacking of parallel G-quadruplexes,<sup>19–22</sup> we propose that in  $\sim 100$  mM  $\text{K}^+$  solution TER18 forms a stacked dimeric G-quadruplex, in which each subunit is a three-layer parallel-stranded G-quadruplex with a cytosine bulge in the second G-tract column (Figure 4). The two subunits in the dimeric G-quadruplex of TER18 are stacked at their 5'-end. Different stacking isomers have been observed previously,<sup>20,22</sup> and only one possible stacking isomer is shown in Figure 4 for illustration purposes. Data supporting the stacking of two G-quadruplex blocks of TER18 include (i) the NMR observation of the RNA concentration-dependent equilibrium described above; (ii) solvent-exchange protection of imino protons, and (iii) gel electrophoresis experiments. These experiments were performed with both TER18 and a modified sequence TER18-2A, in which two adenines were added at the 5'-end to disrupt the stacking between two G-quadruplex blocks.<sup>19,20</sup> TER18-2A was shown by CD and NMR spectroscopy to also form a parallel G-quadruplex (Figures S3 and S4, Supporting Information).

The solvent-exchange experiments on TER18 revealed the protection of 8 imino proton peaks for the form observed at high salt conditions (Figure 5a) but only 4 imino proton peaks for the form observed at low salt conditions (Figure 5b), consistent with the formation of a stacked dimeric G-quadruplex by TER18 at high salt conditions. This solvent protection behavior is in contrast to that observed for the TER18-2A sequence: mainly, only 4 imino protons remained after dissolving TER18-2A in  $\text{D}_2\text{O}$  at both low and high salt conditions (Figure S4, Supporting Information).

We performed a native gel electrophoresis experiment (Figure 6) to probe the molecular size of the G-quadruplex formed by the TER18 sequence in  $\sim 100$  mM  $\text{K}^+$  solution. The migration of TER18 was the same as that of the structure formed by the 10-nt human TERRA sequence r(GGGUAGGGU) involving the stacking of two G-quadruplex blocks,<sup>21,32</sup> which was slower than that of the one-block G-quadruplex formed by the 12-nt human TERRA sequence r(UAGGGUAGGGU).<sup>32</sup> In contrast, the TER18-2A sequence was observed to migrate at the same level as the one-

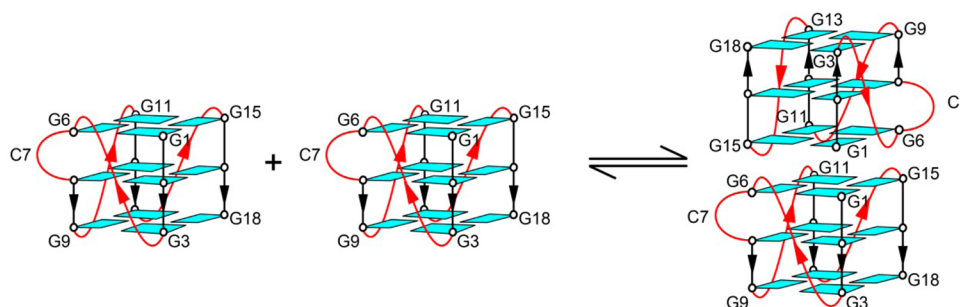


**Figure 4.** Proposed G-quadruplex folding topology and monomer–dimer equilibrium of TER18 in potassium solution.



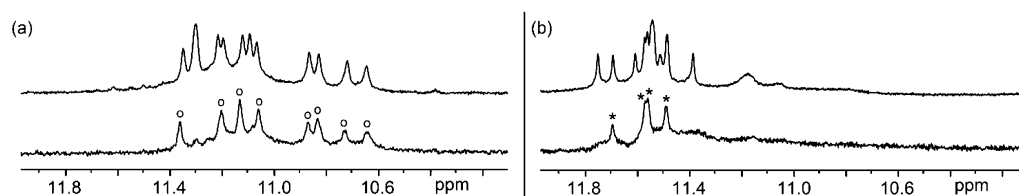


**Figure 5.** Solvent-exchange experiments of G-quadruplexes formed by TER18 in solution containing (a) 70 mM KCl and 20 mM potassium phosphate at pH 7 or (b) 0.5 mM KCl and 0.5 mM potassium phosphate at pH 7. The top spectra are imino proton spectra recorded in 90% H<sub>2</sub>O and 10% D<sub>2</sub>O. The bottom spectra are imino proton spectra of the samples, immediately after dissolving them in D<sub>2</sub>O. Experimental conditions: temperature, 25 °C; RNA concentration, 100  $\mu$ M.

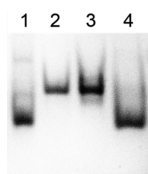


**Figure 6.** Native polyacrylamide gel electrophoresis (PAGE). Lane 1, 12-nt human TERRA sequence, r(UAGGGUAGGGU); lane 2, 10-nt human TERRA sequence, r(GGGUUAGGGU); lane 3, TER18, r(GGGUUGCGGAGGGUGGGC). Lane 4: TER18-2A, r(AAGG-GUUGCGGAGGGUGGGC). The gel was visualized by the UV shadowing method.

block G-quadruplex. These results supported the formation of a stacked dimeric G-quadruplex in TER18, which was disrupted by the addition of the 2A flanking sequence at the 5'-end in TER18-2A.

In conclusion, our data suggest that the first 18-nt of the 5'-terminal region of hTERC can form a stacked dimeric G-quadruplex with bulges in K<sup>+</sup> solution. This structure could be biologically relevant for the dimerization and other interactions of the active human telomerase.<sup>58–61</sup> The extent of the stacked dimer formation can be modulated by 5'-capping of hTERC,<sup>20</sup> while the P1 helix formation should be compatible with and have little effect on this G-quadruplex folding and 5'-end stacking. Although the formation of bulges is expected to reduce G-quadruplex stability,<sup>6</sup> the structure formed by the first 18-nt of hTERC is highly stable exhibiting greater thermal stability than the counterpart formed by a TERRA sequence.

## ■ ASSOCIATED CONTENT

### ● Supporting Information

Additional melting data, CD, and NMR spectra. This material is available free of charge via the Internet at <http://pubs.acs.org>.

## ■ AUTHOR INFORMATION

### Corresponding Author

\*Tel: +65 6514 1915. Fax: +65 6795 7981. E-mail: [phantuan@ntu.edu.sg](mailto:phantuan@ntu.edu.sg)

### Funding

This research was supported by Singapore Ministry of Education and Nanyang Technological University grants to A.T.P.

### Notes

The authors declare no competing financial interest.

## ■ ABBREVIATIONS

TERC, telomerase RNA; NMR, nuclear magnetic resonance; PAGE, polyacrylamide gel electrophoresis; JR, jump-and-return

## ■ REFERENCES

- (1) Davis, J. T. (2004) G-quartets 40 years later: from 5'-GMP to molecular biology and supramolecular chemistry. *Angew. Chem., Int. Ed.* 43, 668–698.
- (2) Burge, S., Parkinson, G. N., Hazel, P., Todd, A. K., and Neidle, S. (2006) Quadruplex DNA: sequence, topology and structure. *Nucleic Acids Res.* 34, 5402–5415.
- (3) Patel, D. J., Phan, A. T., and Kuryavyi, V. (2007) Human telomere, oncogenic promoter and 5'-UTR G-quadruplexes: diverse higher order DNA and RNA targets for cancer therapeutics. *Nucleic Acids Res.* 35, 7429–7455.
- (4) Phan, A. T. (2010) Human telomeric G-quadruplex: structures of DNA and RNA sequences. *FEBS J.* 277, 1107–1117.
- (5) Pan, B., Xiong, Y., Shi, K., and Sundaralingam, M. (2003) Crystal structure of a bulged RNA tetraplex at 1.1 Å resolution: implications for a novel binding site in RNA tetraplex. *Structure* 11, 1423–1430.
- (6) Mukundan, V. T., and Phan, A. T. (2013) Bulges in G-quadruplexes: broadening the definition of G-quadruplex-forming sequences. *J. Am. Chem. Soc.* 135, 5017–5028.
- (7) Phan, A. T., Kuryavyi, V., Gaw, H. Y., and Patel, D. J. (2005) Small-molecule interaction with a five-guanine-tract G-quadruplex structure from the human MYC promoter. *Nat. Chem. Biol.* 1, 167–173.
- (8) Phan, A. T., Kuryavyi, V., Burge, S., Neidle, S., and Patel, D. J. (2007) Structure of an unprecedented G-quadruplex scaffold in the human *c-kit* promoter. *J. Am. Chem. Soc.* 129, 4386–4392.
- (9) Chen, Y., Agrawal, P., Brown, R. V., Hatzakis, E., Hurley, L., and Yang, D. (2012) The major G-quadruplex formed in the human platelet-derived growth factor receptor  $\beta$  promoter adopts a novel broken-strand structure in K<sup>+</sup> solution. *J. Am. Chem. Soc.* 134, 13220–13223.
- (10) Lim, K. W., Amrane, S., Bouaziz, S., Xu, W., Mu, Y., Patel, D. J., Luu, K. N., and Phan, A. T. (2009) Structure of the human telomere in K<sup>+</sup> solution: a stable basket-type G-quadruplex with only two G-tetrad layers. *J. Am. Chem. Soc.* 131, 4301–4309.
- (11) Nielsen, J. T., Arar, K., and Petersen, M. (2009) Solution structure of a locked nucleic acid modified quadruplex: introducing the V4 folding topology. *Angew. Chem., Int. Ed.* 48, 3099–3103.
- (12) Kuryavyi, V., Kettani, A., Wang, W., Jones, R., and Patel, D. J. (2000) A diamond-shaped zipper-like DNA architecture containing triads sandwiched between mismatches and tetrads. *J. Mol. Biol.* 295, 455–469.
- (13) Zhang, N., Gorin, A., Majumdar, A., Kettani, A., Chernichenko, N., Skripkin, E., and Patel, D. J. (2001) V-shaped scaffold: a new architectural motif identified in an A x (G x G x G x G) pentad-containing dimeric DNA quadruplex involving stacked G(anti) x G(anti) x G(anti) x G(syn) tetrads. *J. Mol. Biol.* 311, 1063–1079.
- (14) Kuryavyi, V., Phan, A. T., and Patel, D. J. (2010) Solution structures of all parallel-stranded monomeric and dimeric G-quadruplex scaffolds of the human *c-kit2* promoter. *Nucleic Acids Res.* 38, 6757–6773.
- (15) Kuryavyi, V., and Patel, D. J. (2010) Solution structure of a unique G-quadruplex scaffold adopted by a guanosine-rich human intronic sequence. *Structure* 18, 73–82.

- (16) Trajkovski, M., da Silva, M. W., and Plavec, J. (2012) Unique structural features of interconverting monomeric and dimeric G-quadruplexes adopted by a sequence from the intron of the *N-myc* gene. *J. Am. Chem. Soc.* 134, 4132–4141.
- (17) Marusic, M., Sket, P., Bauer, L., Viglasky, V., and Plavec, J. (2012) Solution-state structure of an intramolecular G-quadruplex with propeller, diagonal and edgewise loops. *Nucleic Acids Res.* 40, 6946–6956.
- (18) Marusic, M., Veedu, R. N., Wengel, J., and Plavec, J. (2013) G-rich VEGF aptamer with locked and unlocked nucleic acid modifications exhibits a unique G-quadruplex fold. *Nucleic Acids Res.* 41, 9524–9536.
- (19) Do, N. Q., Lim, K. W., Teo, M. H., Heddi, B., and Phan, A. T. (2011) Stacking of G-quadruplexes: NMR structure of a G-rich oligonucleotide with potential anti-HIV and anticancer activity. *Nucleic Acids Res.* 39, 9448–9457.
- (20) Do, N. Q., and Phan, A. T. (2012) Monomer-dimer equilibrium for the 5'-5' stacking of propeller-type parallel-stranded G-quadruplexes: NMR structural study. *Chem. Eur. J.* 18, 14752–14759.
- (21) Martadinata, H., and Phan, A. T. (2013) Structure of human telomeric RNA (TERRA): stacking of two G-quadruplex blocks in K<sup>+</sup> solution. *Biochemistry* 52, 2176–2183.
- (22) Kuryavyi, V., Cahoon, L. A., Seifert, H. S., and Patel, D. J. (2012) RecA-binding *pilE* G4 sequence essential for pilin antigenic variation forms monomeric and 5' end-stacked dimeric parallel G-quadruplexes. *Structure* 20, 2090–2102.
- (23) Borbone, N., Amato, J., Oliviero, G., D'Atri, V., Gabelica, V., De Pauw, E., Piccialli, G., and Mayol, L. (2011) d(CGGTGGT) forms an octameric parallel G-quadruplex via stacking of unusual G(:C):G(:C):G(:C):G(:C) octads. *Nucleic Acids Res.* 39, 7848–7857.
- (24) Majumdar, A., and Patel, D. J. (2002) Identifying hydrogen bond alignments in multistranded DNA architectures by NMR. *Acc. Chem. Res.* 35, 1–11.
- (25) Webba da Silva, M. (2003) Association of DNA quadruplexes through G:C:G:C tetrads. Solution structure of d(GCGGTGGAT). *Biochemistry* 42, 14356–14365.
- (26) Krishnan-Ghosh, Y., Liu, D., and Balasubramanian, S. (2004) Formation of an interlocked quadruplex dimer by d(GGGT). *J. Am. Chem. Soc.* 126, 11009–11016.
- (27) Phan, A. T., Kuryavyi, V., Ma, J. B., Faure, A., Andréola, M. L., and Patel, D. J. (2005) An interlocked dimeric parallel-stranded DNA quadruplex: a potent inhibitor of HIV-1 integrase. *Proc. Natl. Acad. Sci. U.S.A.* 102, 634–639.
- (28) Phan, A. T., and Do, N. Q. (2013) Engineering of interlocked DNA G-quadruplexes as a robust scaffold. *Nucleic Acids Res.* 41, 2683–2688.
- (29) Pan, B., Shi, K., and Sundaralingam, M. (2006) Base-tetrad swapping results in dimerization of RNA quadruplexes: implications for formation of the i-motif RNA octaplex. *Proc. Natl. Acad. Sci. U.S.A.* 103, 3130–3134.
- (30) Xu, Y., Kaminaga, K., and Komiyama, M. (2008) G-quadruplex formation by human telomeric repeats-containing RNA in Na<sup>+</sup> solution. *J. Am. Chem. Soc.* 130, 11179–11184.
- (31) Xu, Y., Ishizuka, T., Kimura, T., and Komiyama, M. (2010) A U-tetrad stabilizes human telomeric RNA G-quadruplex structure. *J. Am. Chem. Soc.* 132, 7231–7233.
- (32) Martadinata, H., and Phan, A. T. (2009) Structure of propeller-type parallel-stranded RNA G-quadruplexes, formed by human telomeric RNA sequences in K<sup>+</sup> solution. *J. Am. Chem. Soc.* 131, 2570–2578.
- (33) Collie, G. W., Haider, S. M., Neidle, S., and Parkinson, G. N. (2010) A crystallographic and modelling study of a human telomeric RNA (TERRA) quadruplex. *Nucleic Acids Res.* 38, 5569–5580.
- (34) Mashima, T., Matsugami, A., Nishikawa, F., Nishikawa, S., and Katahira, M. (2009) Unique quadruplex structure and interaction of an RNA aptamer against bovine prion protein. *Nucleic Acids Res.* 37, 6249–6258.
- (35) Phan, A. T., Kuryavyi, V., Darnell, J. C., Serganov, A., Majumdar, A., Ilin, S., Raslin, T., Polonskaia, A., Chen, C., Clain, D., Darnell, R. B., and Patel, D. J. (2011) Structure-function studies of FMRP RGG peptide recognition of an RNA duplex-quadruplex junction. *Nat. Struct. Mol. Biol.* 18, 796–804.
- (36) Lipps, H. J., and Rhodes, D. (2009) G-quadruplex structures: in vivo evidence and function. *Trends Cell Biol.* 19, 414–422.
- (37) Cahoon, L. A., and Seifert, H. S. (2009) An alternative DNA structure is necessary for pilin antigenic variation in *Neisseria gonorrhoeae*. *Science* 325, 764–767.
- (38) Lopes, J., Piazza, A., Bermejo, R., Kriegsmann, B., Colosio, A., Teulade-Fichou, M. P., Foiani, M., and Nicolas, A. (2011) G-quadruplex-induced instability during leading-strand replication. *EMBO J.* 30, 4033–4046.
- (39) Maizels, N., and Gray, L. T. (2013) The G4 genome. *PLoS Genet.* 9, e1003468.
- (40) Biffi, G., Di Antonio, M., Tannahill, D., and Balasubramanian, S. (2014) Visualization and selective chemical targeting of RNA G-quadruplex structures in the cytoplasm of human cells. *Nat. Chem.* 6, 75–80.
- (41) Greider, C. W., and Blackburn, E. H. (1985) Identification of a specific telomere terminal transferase activity in *Tetrahymena* extracts. *Cell* 43, 405–413.
- (42) Kim, N. W., Piatyszek, M. A., Prowse, K. R., Harley, C. B., West, M. D., Ho, P. L., Coviello, G. M., Wright, W. E., Weinrich, S. L., and Shay, J. W. (1994) Specific association of human telomerase activity with immortal cells and cancer. *Science* 266, 2011–2015.
- (43) Greider, C. W., and Blackburn, E. H. (1987) The telomere terminal transferase of *Tetrahymena* is a ribonucleoprotein enzyme with two kinds of primer specificity. *Cell* 51, 887–898.
- (44) Feng, J., Funk, W. D., Wang, S. S., Weinrich, S. L., Avilion, A. A., Chiu, C. P., Adams, R. R., Chang, E., Allsopp, R. C., Yu, J., et al. (1995) The RNA component of human telomerase. *Science* 269, 1236–1241.
- (45) Jiang, J., Miracco, E. J., Hong, K., Eckert, B., Chan, H., Cash, D. D., Min, B., Zhou, Z. H., Collins, K., and Feigon, J. (2013) The architecture of *Tetrahymena* telomerase holoenzyme. *Nature* 496, 187–192.
- (46) Sauerwald, A., Sandin, S., Cristofari, G., Scheres, S. H., Lingner, J., and Rhodes, D. (2013) Structure of active dimeric human telomerase. *Nat. Struct. Mol. Biol.* 20, 454–460.
- (47) Wenz, C., Enenkel, B., Amacker, M., Kelleher, C., Damm, K., and Lingner, J. (2001) Human telomerase contains two cooperating telomerase RNA molecules. *EMBO J.* 20, 3526–3534.
- (48) Alves, D., Li, H., Codrington, R., Orte, A., Ren, X., Klennerman, D., and Balasubramanian, S. (2008) Single-molecule analysis of human telomerase monomer. *Nat. Chem. Biol.* 4, 287–289.
- (49) Chen, J. L., Blasco, M. A., and Greider, C. W. (2000) Secondary structure of vertebrate telomerase RNA. *Cell* 100, 503–514.
- (50) Zhang, Q., Kim, N. K., and Feigon, J. (2011) Architecture of human telomerase RNA. *Proc. Natl. Acad. Sci. U.S.A.* 108, 20325–20332.
- (51) Li, X., Nishizuka, H., Tsutsumi, K., Imai, Y., Kurihara, Y., and Uesugi, S. (2007) Structure, interactions and effects on activity of the 5'-terminal region of human telomerase RNA. *J. Biochem.* 141, 755–765.
- (52) Gros, J., Guédin, A., Mergny, J. L., and Lacroix, L. (2008) G-Quadruplex formation interferes with P1 helix formation in the RNA component of telomerase hTerc. *ChemBioChem* 9, 2075–2079.
- (53) Sexton, A. N., and Collins, K. (2011) The 5' guanosine tracts of human telomerase RNA are recognized by the G-quadruplex binding domain of the RNA helicase DHX36 and function to increase RNA accumulation. *Mol. Cell. Biol.* 31, 736–743.
- (54) Lattmann, S., Stadler, M. B., Vaughn, J. P., Akman, S. A., and Nagamine, Y. (2011) The DEAH-box RNA helicase RHAU binds an intramolecular RNA G-quadruplex in TERC and associates with telomerase holoenzyme. *Nucleic Acids Res.* 39, 9390–9404.
- (55) Booy, E. P., Meier, M., Okun, N., Novakowski, S. K., Xiong, S., Stetefeld, J., and McKenna, S. A. (2011) The RNA helicase RHAU (DHX36) unwinds a G4-quadruplex in human telomerase RNA and promotes the formation of the P1 helix template boundary. *Nucleic Acids Res.* 40, 4110–4124.

- (56) Phan, A. T., Guéron, M., and Leroy, J. L. (2001) Investigation of unusual DNA motifs. *Methods Enzymol.* 338, 341–371.
- (57) Adrian, M., Heddi, B., and Phan, A. T. (2012) NMR spectroscopy of G-quadruplexes. *Methods* 57, 11–24.
- (58) Prescott, J., and Blackburn, E. H. (1997) Functionally interacting telomerase RNAs in the yeast telomerase complex. *Genes Dev.* 11, 2790–2800.
- (59) Mitchell, J. R., and Collins, K. (2000) Human telomerase activation requires two independent interactions between telomerase RNA and telomerase reverse transcriptase. *Mol. Cell* 6, 361–371.
- (60) Ren, X., Gavory, G., Li, H., Ying, L., Klenerman, D., and Balasubramanian, S. (2003) Identification of a new RNA:RNA interaction site for human telomerase RNA (hTR): structural implications for hTR accumulation and a dyskeratosis congenita point mutation. *Nucleic Acids Res.* 31, 6509–6515.
- (61) Ly, H., Xu, L., Rivera, M. A., Parslow, T. G., and Blackburn, E. H. (2003) A role for a novel ‘trans-pseudoknot’ RNA-RNA interaction in the functional dimerization of human telomerase. *Genes Dev.* 17, 1078–1083.